CHEMISTRY OF MATERIALS
Article

Chem. Mater. **2011,** *23,* 929–934 929
DOI:10.1021/cm101519s

Fast Synthesis of MOF-5 Microcrystals Using Sol−Gel SiO_2 Nanoparticles

Dario Buso,*[,†,‡] Kate M. Nairn,[†] Michele Gimona,[†] Anita J. Hill,[†] and Paolo Falcaro*[,†]

[†]*CSIRO, Materials Science and Engineering, Locked Bag 33, Clayton Sth MDC, VIC 3169, Australia, and* [‡]*Centre for Micro-Photonics and CUDOS, Faculty of Engineering and Industrial Sciences, Swinburne University of Technology, PO Box 218, Hawthorn, VIC 3122, Australia*

Received May 31, 2010. Revised Manuscript Received November 29, 2010

The work reports on the synthesis of an archetypal metal organic framework (MOF-5) microcrystals with a narrow size distribution using SiO_2 nanoparticles with tailored surface chemistry as nucleating agents. The nanoparticles boost the reaction rate by up to an order of magnitude compared to the conventional MOF-5 solvothermal synthesis and can be successfully used as nucleation seeds for the selective growth of MOF-5 on specific substrates. These results are important fundamental advances toward the controlled scale-up of MOF synthesis and directed MOF growth on suitable supports.

Introduction

Metal organic frameworks (MOFs) are an emerging class of hybrid material where metal ions or small inorganic nanoclusters are linked into one-, two-, or three-dimensional networks by multifunctional organic linkers.[1,2] A variety of open micro- and mesoporous structures can be developed, leading to materials with extreme surface area, in some cases with reported measured values up to 5900 m^2/g.[3] Moreover, the possibility to arbitrarily engineer the cavity architecture and the pore surface chemistry makes MOFs strong candidates for a wide variety of applications, from gas storage/separation[4−6] to catalysis,[7] drug delivery,[8] optoelectronics,[9] and sensing.[10]

The number of studies of MOF chemical structures and properties is overwhelming; however, only a small number of reports investigate MOF formation mechanisms, as making direct in situ measurements of nucleation and growth is difficult. Knowledge of formation mechanisms is extremely valuable to tailor MOF properties and also from a process engineering perspective to scale-up MOF production for future industrial application. The generally accepted mechanism for MOF formation in solution is based upon the homogeneous nucleation of secondary building units (SBUs),[11] which in turn join together to form the final crystal structure.[12,13] In situ AFM measurements[14] have suggested that, in addition to the junction of SBUs, MOF growth proceeds by a two-dimensional surface nucleation "birth and spread" mechanism.[14,15] This mechanism involves the addition of much smaller building units to the MOF surface and may be more relevant to the overall rate of crystal formation and the final MOF morphology.[16] Surfaces capable of promoting and directing MOF growth can provide a route to fabrication of functional devices on a large scale.

Fischer and co-workers[13,17,18] have shown directed MOF growth on 2D surfaces functionalized with self-assembled carboxy-terminated monolayers (SAMs). In their approach, SBUs or larger MOF-5 nuclei bind to Zn^{2+} cations coordinated on the carboxylated SAMs via a terephthalate bridge. From an engineering perspective, this approach is an important step toward the development of MOF-5-based solid state devices and thin films. On the other hand, for large scale production purposes, the protocol is time-expensive requiring more than 100 h preparation

*To whom correspondence should be addressed. E-mail: dario.buso@csiro.au (D.B.); paolo.falcaro@csiro.au (P.F.).

(1) Chae, H. K.; Siberio-Perez, D. Y.; Kim, J.; Go, Y.; Eddaoudi, M.; Matzger, A. J.; O'Keeffe, M.; Yaghi, O. M. *Nature* **2004**, *427*, 523.
(2) Eddaoudi, M.; Kim, J.; Rosi, N.; Vodak, D.; Wachter, J.; O'Keeffe, M.; Yaghi, O. M. *Science* **2002**, *295*, 469.
(3) Férey, G.; Mellot-Draznieks, C.; Serre, C.; Millange, F.; Dutour, J.; Surble, S.; Margiolaki, I. *Science* **2005**, *309*, 2040.
(4) Fang, Q. R.; Zhu, G. S.; Jin, Z.; Ji, Y. Y.; Ye, J. W.; Xue, M.; Yang, H.; Wang, Y.; Qiu, S. H. *Angew. Chem., Int. Ed.* **2007**, *46*, 6638.
(5) Zlotea, C.; Campesi, R.; Cuevas, F.; Leroy, E.; Dibandjo, P.; Volkringer, C.; Loiseau, T.; Férey, G.; Latroche, M. *J. Am. Chem. Soc.* **2010**, *132*, 2991.
(6) Liu, Y.; Ng, Z.; Khan, E. A.; Jeong, H. K.; Ching, C. B.; Lai, Z. *Microporous Mesoporous Mater.* **2009**, *118*, 296.
(7) Proch, S.; Herrmannsdörfer, J.; Kempe, R.; Kern, C.; Jess, A.; Seyfarth, L.; Senker, J. *Chem.—Eur. J.* **2008**, *14*, 8204.
(8) Cohen, S. M. *Curr. Opin. Chem. Biol.* **2007**, *11*, 115.
(9) Winston, E. B.; Lowell, P. J.; Vacek, J.; Chocholoušová, J.; Michl, J.; Price, J. C. *Phys. Chem. Chem. Phys.* **2008**, *10*, 5188.
(10) Achmann, S.; Hagen, G.; Kita, J.; Malkowsky, I. M.; Kiener, C.; Moos, R. *Sensors* **2009**, *9*, 1574.
(11) Eddaoudi, M.; Li, H. L.; Yaghi, O. M. *J. Am. Chem. Soc.* **2000**, *122*, 1391.
(12) Millange, F.; Medina, M. I.; Guillou, N.; Férey, G.; Golden, K. M.; Walton, R. I. *Angew. Chem., Int. Ed.* **2010**, *49*, 763.
(13) Hermes, S.; Schröder, F.; Chelmovski, R.; Wöll, C.; Fischer, R. A. *J. Am. Chem. Soc.* **2005**, *127*, 13744.
(14) Shoaee, M.; Anderson, M. W.; Attfield, M. P. *Angew. Chem., Int. Ed.* **2008**, *47*, 8525.
(15) Mullin, J. W. *Crystallization*; Elsevier Butterworth-Heinemann: Oxford, 2001; pp 216−288.
(16) Morris, R. E. *Chem. Phys. Chem.* **2009**, *10*, 327.
(17) Hermes, S.; Zacher, D.; Baunemann, A.; Wöll, C.; Fisher, R. A. *Chem. Mater.* **2007**, *19*, 2168.
(18) Shekhah, O.; Wang, H.; Paradinas, M.; Ocal, C.; Schüpbach, B.; Terfort, A.; Zacher, D.; Fisher, R. A.; Wöll, C. *Nat. Mater.* **2009**, *8*, 481.

time. In addition, the amount of MOF-5 that forms is limited by the planar surface area on which the SAM is deposited.

In the present work, we extend the surface-driven MOF growth from 2D to 3D surfaces, introducing a procedure to produce MOF-5 by nucleation on modified SiO_2 spherical nanoparticles (NPs) suspended in the MOF growing medium. Strategically, our sol−gel approach provides a promising route toward the large-scale production of colloidal MOFs by leveraging the enormous surface areas offered by nanosized seeds to nucleate MOFs. An additional industrial advantage of our synthetic route lies in the exploitation of a heterogeneous MOF formation mechanism, hence providing faster nucleation kinetics. The observed MOF-5 crystal formation rate is over 10 times faster than with the conventional solvothermal approach, allowing for MOF-5 production within a few hours. The faster production rate at a substantially lower cost is an important step toward the effective scale-up of MOF production. Although also microwave-assisted MOF synthesis shows remarkable formation rates,[19,20] the synthesis of SiO_2 NPs can easily complement an industrial production line, as it is performed at room temperature and is cheap and considerable volumes of NP suspensions can be produced in a short time.

The SiO_2 NP mediated synthesis of MOF-5 seems to be a typical nucleation-controlled process, producing small crystals with a narrow size distribution; at the same time, the proposed synthesis does not rely on growth limiting surface agents (as used recently to produce nanoparticles of another MOF, MIL-89[21]). The MOF crystals produced are, hence, excellent candidate substrates for scaled-up MOF production and also for production of other frameworks. Moreover, the surface modified SiO_2 nanoparticles can be successfully used as nucleation seeds for the selective growth of MOF-5 on specific substrates with no need for substrate prefunctionalization. These results are important fundamental advances toward the controlled scale-up of MOF synthesis and directed MOF growth on suitable supports for device fabrication.

Materials and Methods

Tetraethoxysilane (TEOS), aminopropyl triethoxysilane (APTES), vinyl trimethoxysilane (VTES), fluorescein-isothiocyanate (FITC), zinc nitrate hexahydrate, 1,4-benzenecarboxylic acid (BCA), diethylformamide (DEF), and dimethylformamide (DMF) have been purchased from Aldrich and used without further purification. Functional SiO_2 NPs have been synthesized using a modified sol−gel Stöber approach.[22] When a suitable alkoxysilane precursor to the main reaction batch was added, it had been possible to obtain NPs with different chemical functionality. Particles with amino, carboxy, and hydroxy functional groups have been obtained using APTES,[23] oxidized VTES,[24] and FITC,[25] respectively.

SiO_2 Particles (167 nm size). TEOS (4.5 mL) was first dissolved in EtOH (45 mL), and subsequently, a 25% ammonia solution (5 mL) was added dropwise under continuous and vigorous stirring. After 60 min, the solution started to assume an opalescent tone due to scattering from the forming SiO_2 nanoparticles. The mixture was stirred overnight to allow for complete reaction of the precursors. The suspended particles were centrifuged, vacuum-dried, and resuspended in fresh EtOH. The washing procedure was repeated four times, and the particles were finally stored as a dry white powder. The whole procedure was performed under room conditions.

SiO_2−NH_2 Particles (197 nm size). TEOS (4.08 mL) and APTES (0.42 mL) were first dissolved in EtOH (45 mL). Subsequently, a 25% ammonia solution (5 mL) was added dropwise under continuous and vigorous stirring. The mixture was allowed to react overnight, and the particles were eventually washed according to the same procedure described above. The particles were stored as a white dry powder.

SiO_2−COOH Particles (153 nm size). TEOS (4.08 mL) and VTES (0.42 mL) were initially dissolved in EtOH (45 mL). Subsequently, a 25% ammonia solution (5 mL) was added dropwise under continuous and vigorous stirring. The mixture was allowed to react overnight, and the particles were eventually washed as described above.

The vinyl terminations of VTES have then been oxidized to carboxy-functions by suspending the particles into an aqueous solution (40 mL) of $KMnO_4$ (4 mg) and $NaIO_4$ (168 mg) for 12 h, according to a protocol described by Wasserman and coworkers.[24] Again, the colloids have been separated by centrifugation and washed twice with distilled water and EtOH.

SiO_2−OH Particles (197 nm size). Some of the SiO_2−NH_2 NPs were suspended in a solution of FITC (7 mg) in EtOH (15 mL). The iso-thiocyanate termination of the FITC molecules condenses with the amino functions of the NPs, exposing the hydroxy terminations of the FITC molecules to the solvent.[25] The particles have been kept suspended in the FITC solution for 20 min, then centrifuged, and washed in fresh EtOH twice, to be finally vacuum-dried and stored as an orange powder.

Solvothermal Growth of MOF-5 in the Presence of SiO_2 NPs. MOF-5 crystals were synthesized using a typical solvothermal approach.[6] A mother batch of precursors was first synthesized dissolving $Zn(NO_3)_2$ (1.32 g) and BCA (0.15 g) in DEF (35 mL). The resulting solution was then divided into 3.5 mL aliquots: one for each of the surface modified NP types, plus a control (five aliquots in total). Fifteen milligrams of SiO_2 NPs with different functionalities was added to each one of the aliquots, and the mixture was suspended in an ultrasonic bath for 30 min. No particles were added to the control solution. The vials were Teflon-sealed and heated at 95 °C under constant stirring for up to 10 h.

MOF-5 Growth on a Bed of SiO_2 NPs. A circular bed of SiO_2−COOH NPs was formed on a silicon wafer by drop-casting a concentrated NP suspension in EtOH, which was subsequently vacuum-dried overnight at 1 mbar. The modified silicon substrate was then immersed into a MOF-5 precursor

(19) Lu, C. M.; Liu, J.; Xiao, K.; Harris, A. T. *Chem. Eng. J.* **2010**, *156*, 465.
(20) Choi, J. S.; Son, W. J.; Kim, J.; Ahn, W. S. *Microporous Mesoporous Mater.* **2008**, *116*, 727.
(21) Horcajada, P.; Serre, C.; Grosso, D.; Boissiere, C.; Perruchas, S.; Sanchez, C.; Ferey, G. *Adv. Mater.* **2009**, *21*, 1931.
(22) Brinker, C. J.; Scherer, G. W. *Sol-Gel Science: the Physics and Chemistry of Sol-Gel Processing*; Academic Press Inc.: New York, 1990.
(23) Buso, D.; Palmer, L.; Bello, V.; Mattei, G.; Post, M.; Mulvaney, P.; Martucci, A. *J. Mater. Chem.* **2009**, *19*(14), 2051.
(24) Wasserman, S. R.; Tao, Y. T.; Whitesides, G. M. *Langmuir* **1989**, *5*, 1074.
(25) Falcaro, P.; Malfatti, L.; Vaccari, L.; Amenitsch, H.; Marmiroli, B.; Grenci, G.; Innocenzi, P. *Adv. Mater.* **2009**, *21*, 4932.

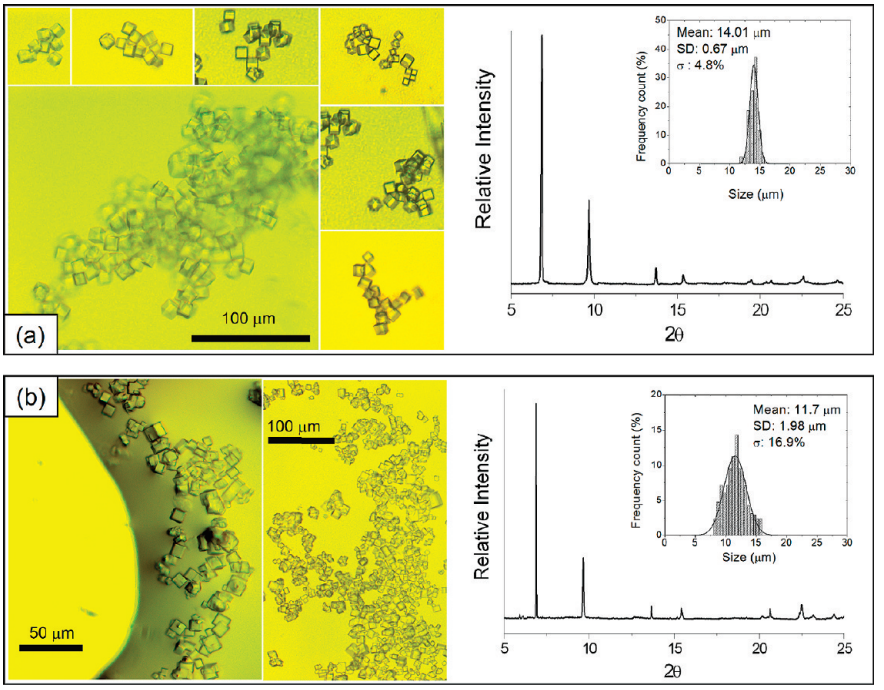

Figure 1. (a) Optical microscopy images, XRD pattern, and crystal size/size distribution diagram of MOF-5 obtained by adding SiO_2−COOH NPs to the MOF-5 precursor solution, after 10 h at 95 °C. (b) Optical microscope images, XRD pattern, and crystal size/size distribution diagram of MOF-5 crystals formed in the presence of SiO_2−NH_2 NPs after a 10 h reaction at 95 °C. The optical images were taken by drop casting the crystal suspension onto a glass microscope slide, while the XRD patterns were measured on vacuum and temperature dried MOF-5 crystals.

solution obtained according to the procedure described above, with the only difference that DMF was used as the solvent instead of DEF. The batch was then Teflon-sealed and immersed into an oil bath previously heated at 95 °C. The substrates have been extracted after a 2 h reaction, rinsed with fresh DMF, and vacuum-dried prior to further analysis.

Results and Discussion

Several batches of SiO_2 NPs have been synthesized using a modified Stöber approach. Besides pure SiO_2 NPs, suitable sol−gel precursors have been used to produce chemically modified NP suspensions with amino, carboxy, and hydroxy groups added to the main SiO_2 network (see Materials and Methods for details). FTIR analysis of dried NP powders confirmed the presence of these functional groups within the SiO_2 network (see Supporting Information). The modified Stöber protocol reported here allowed for the fast synthesis of highly concentrated SiO_2 NP suspensions. In addition to the elevated amount of NPs produced, this approach is appealing from an industrial perspective also for its intrinsic simplicity, speed, and high reaction yield. Furthermore, the high degree of compositional control makes it possible to produce particles with customized functionality. Such NP dispersions are the three-dimensional extension of the 2D growth surfaces concept reported by Fischer's group[26] and provide a dramatic increase in the overall area suitable for MOF growth. The present work also further extends the study of MOF growth on functionalized supports with amino-terminated species, not yet reported in literature.

The SiO_2 NPs have subsequently been suspended in several MOF-5 growing media containing zinc nitrate and 1,4-benzenecarboxylic acid dissolved in *N*,*N*-diethylformamide (DEF). All the solutions underwent sonication until completely transparent. The vials with the suspensions were then inserted into an oil heated holder at 95 °C and kept under constant stirring according to the usual solvothermal procedure adopted for the synthesis of MOF-5.[6] After 2 hours into the reaction, the growing media containing SiO_2−COOH and SiO_2−NH_2 NPs show an obvious decrease in transparency as a thick suspension starts to form (see Supporting Information).

After a 10 h reaction at 95 °C, optical microscopy images (Figure 1) reveal the presence of cubic crystals formed in the solutions containing SiO_2−COOH and SiO_2−NH_2 NPs. The XRD patterns shown in Figure 1a,b are consistent with that reported for MOF-5.[27] The main diffraction peaks at low angles, $2\theta = 6.9°$ (⟨200⟩ plane, $d = 12.8$ Å) and 9.7° (⟨220⟩ plane, $d = 9.1$ Å), are indicative of the modular arrangement of large pores in the MOF-5 cubic lattice. No MOF-5 crystals were observed in the control solution or in the solutions containing SiO_2 and SiO_2−OH NPs in the initial 24 h of reaction. The average size of the crystals promoted by SiO_2−COOH NPs is 14.0 μm with 4.8% size dispersion, while SiO_2−NH_2 promoted cubic crystals with an average size of 11.7 μm and 17% size dispersion.

X-ray diffraction measurements give additional information beyond confirmation that the observed crystals are indeed MOF-5. As an archetype of a typical MOF

(26) Zacher, D.; Shekhah, O.; Woll, C.; Fischer, R. A. *Chem. Soc. Rev.* **2009**, *38*, 1418.

(27) Yaghi, O. M.; Eddaoudi, M.; Li, H.; Kim, J.; Rosi, N. U.S. Patent WO 02/088148, 2002.

structure, MOF-5 has been synthesized via a variety of methods and characterized in extreme detail in countless publications. Hafizovic and co-workers[28] found and confirmed important qualitative correlations between the XRD plots generated by MOF-5 samples and their crystalline quality; their study aimed to explain the wide range of MOF-5 specific surface values reported in the literature, which vary from lows of 722 m^2/g[29] to highs of 3400 m^2/g.[27] It was found that the relative intensities of the 6.9° and 9.7° diffraction signals are strongly affected by the presence of lattice defects, adsorbed species (solvent molecules included), and unreacted Zn centers. As those peaks are the direct evidence of the large MOF-5 pore arrangements, the authors outlined a qualitative relationship between the diffraction plots and the structural quality of MOF-5. Chen and co-workers[30] have recently extended this analysis correlating the intensity of the diffraction peak at 13.8° (⟨400⟩ plane, $d = 6.4$ Å) to the extent of crystal interpenetration. On this basis, our measured diffraction plots show the features typical of high quality and noninterpenetrated MOF-5 crystals, as the relative intensities of the low angle peaks are consistent with the simulated plots (see Supporting Information) and with the analysis presented in refs 28 and 30.

Figure 2 shows SEM images of MOF-5 crystals after a 4 h reaction at 95 °C in the presence of SiO_2−COOH NPs. The samples for imaging have been prepared by fixing dry crystals on the surface of double-sided carbon conductive tape (SPI Supplies) and then coating them with an iridium layer. The crystals in Figure 2a−c were not filtered from the NP suspension, and hence, the images give insight into the interaction between NPs and forming MOF, as the NPs are clearly embedded, or in the process of being embedded, inside the crystal framework; in particular, Figure 2c directly shows several NPs embedded into the forming cube. This is the first evidence of the nucleating effect of the functionalized NPs in the formation of MOF-5 microcrystals. No crystals were observed in the control batch or in those containing SiO_2 and SiO_2−OH NPs.

The SEM images of Figure 3 show a filtered MOF-5 crystal grown in the presence of SiO_2−COOH NPs for 10 h (Figure 3a) and MOF-5 crystals of similar size collected from the control solution after about a 60 h reaction at 95 °C (Figure 3b). The plots of Figure 3c−e show the energy dispersive X-ray (EDAX) signals recorded scanning the imaged crystals and the background tape. Both the plots in Figure 3c,d (control) show distinctive emissions of the MOF-5 components, carbon Kα (0.277 keV), oxygen Kα (0.523 keV), and zinc Lα (1.012 keV). However, in contrast to the plot in Figure 3d (control), the plot in Figure 3c shows the distinctive Kα emission of silicon (1.74 keV), which can be directly associated with the SiO_2 NPs within the MOF-5 structure. The background emission

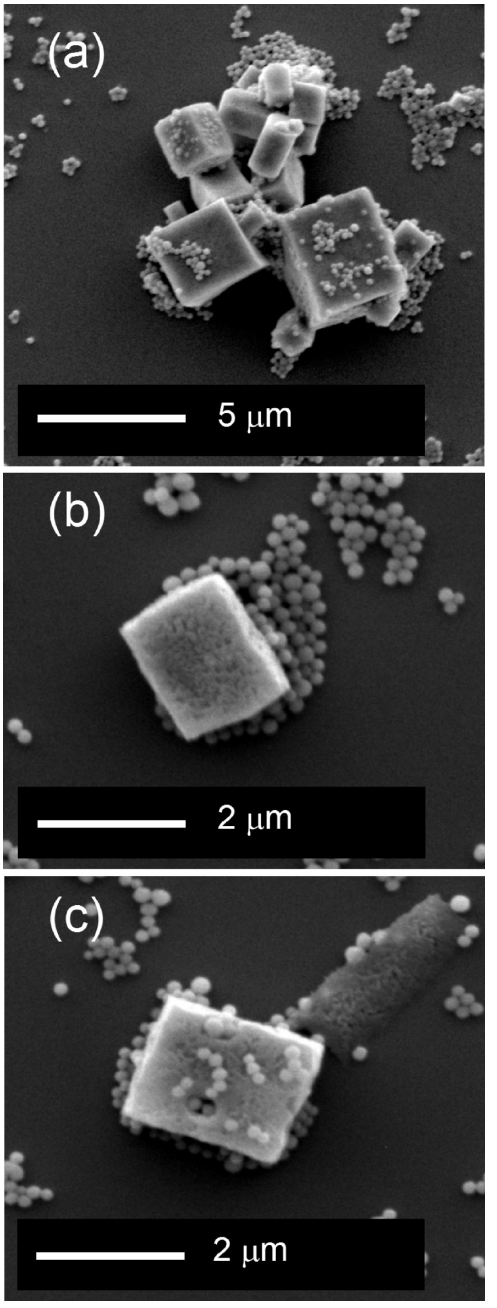

Figure 2. SEM images of MOF-5 crystals formed in a solution containing SiO_2−COOH NPs (a,b) and SiO_2−NH_2 NPs (c) after a 4 h reaction at 95 °C.

(Figure 3e) is dominated by C−Kα and O−Kα emissions. All spectra contain a contribution at 1.978 keV from the Mα emission of the iridium coating.

After observing the seeding effect in solution, the nucleating capability of the modified SiO_2 NPs has also been tested on flat silicon substrates, which are known to be unfavorable supports for MOF-5 growth.[26] SiO_2−COOH modified NPs have been used to illustrate the seeding effect of dry NPs for the production of MOF-5 crystals on 2D surfaces. SiO_2−COOH NPs were selected as the preferred candidates given their superior seeding performance in suspension. In addition, to further extend the method's applicability, the conventional MOF-5 growing medium was synthesized

(28) Hafizovic, J.; Bjørgen, M.; Olsbye, U.; Dietzel, P. D. C.; Bordiga, S.; Prestipino, C.; Lamberti, C.; Lillerud, K. P. *J. Am. Chem. Soc.* **2007**, *129*, 3612.
(29) Huang, L.; Wang, H.; Chen, J.; Wang, Z.; Sun, J.; Zhao, D.; Yan, Y. *Microporous Mesoporous Mater.* **2003**, *58*, 105.
(30) Chen, B.; Wang, X.; Zhang, Q.; Xi, X.; Cai, J.; Qi, H.; Shi, S.; Wang, J.; Yuan, D.; Fang, M. *J. Mater. Chem.* **2010**, *20*, 3758.

using dimethylformamide (DMF) instead of diethylformamide (DEF), which is an appealing choice from an industrial perspective given the substantially lower cost of DMF.

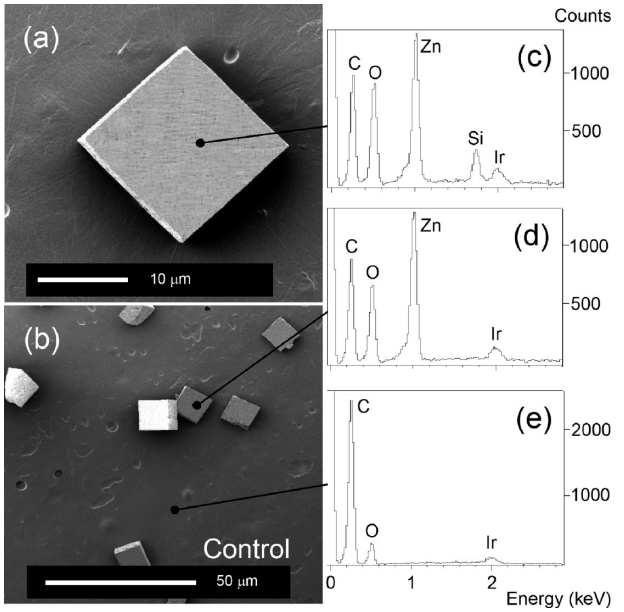

Figure 3. (a) SEM image of a MOF-5 crystal formed in the presence of SiO_2−COOH NPs after a 10 h reaction at 95 °C. (b) SEM image of MOF-5 crystals formed in the control solution (with no NPs) after a 60 h reaction at 95 °C. (c, d, e) EDAX plots measured scanning the crystal of image (a), a crystal of image (b), and the background of image (b), respectively. Note the signal of Si species in the plot (c) indicating the presence of the SiO_2−COOH NPs inside the crystal.

A NP bed on a silicon wafer (see Materials and Methods for details) has been used as a growing medium for MOF-5, and the process has been monitored with FTIR. The experimental steps are shown schematically in Figure 4a. Before MOF growth, the dried NP bed was chemically mapped, as shown in Figure 4b. The siliceous nature of the seeds was confirmed (Si−O−Si silica bonds in the 1200−1000 cm^{-1} region) as well as the twin frequencies of the antisymmetric OCO (ν_a^{OCO}) stretches of the carboxylic terminations, at 1610 cm^{-1} and 1400 cm^{-1}.[31] Compared to SAMs, beds of functionalized SiO_2 NPs provide a higher concentration of −COOH functions, enough to be detected by transmission FTIR. The signal at 1610 cm^{-1} is typical of deprotonated and uncoordinated O−C−O groups,[31,32] further confirmed by the absence of the symmetric stretch of C=O bonds (ν^{CO}) in the 1700−1750 cm^{-1} region. Given the highly basic synthesis conditions of the NPs, these observations are consistent with reported pK_a values for terminal carboxyl functions, which typically range from 2.5 to 6.[33] The maps in Figure 4c show the integrated absorbance of characteristic MOF-5 structural bonds recorded from two different spots of the same sample. The pictures on the left of Figure 4c are optical images of the sampled areas. Once immersed in the MOF-5 growing medium, the unprotonated carboxyls facilitate the coordination of Zn^{2+} cations,

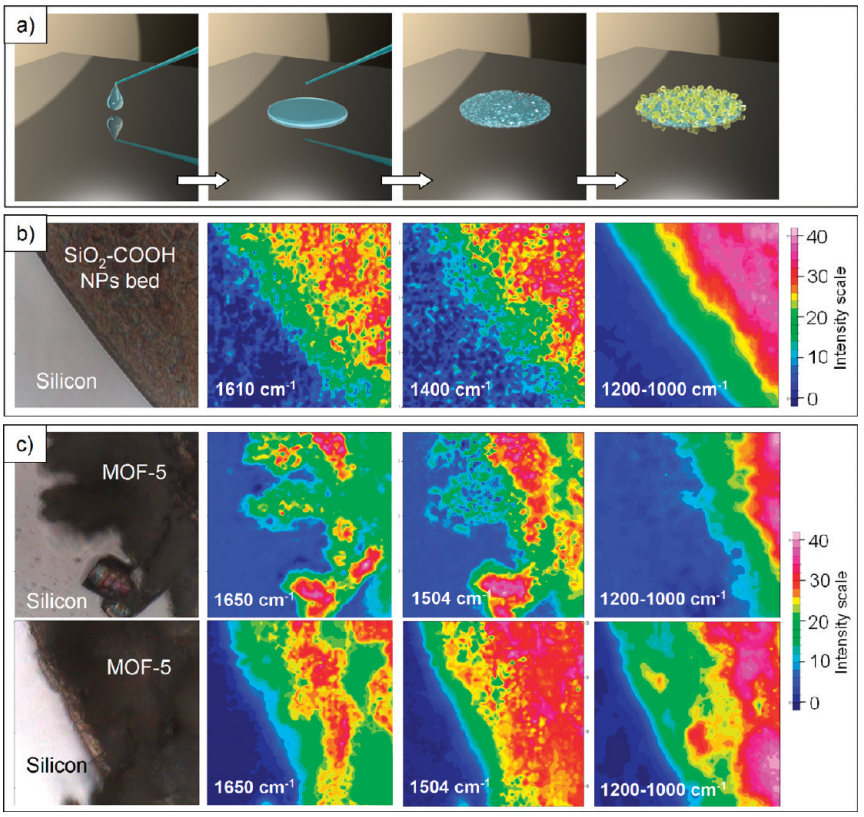

Figure 4. (a) Schematic representation of the experiment executed to test the capability of modified SiO_2 NPs to induce MOF-5 formation on a silicon surface. (b) Optical image and FTIR chemical maps of a bed of SiO_2−COOH NPs dried on a silicon substrate. The chemical maps show the spatial distribution of the NPs and the uncoordinated carboxy groups. (c) Optical images and FTIR chemical maps of MOF-5 crystals grown locally on the SiO_2−COOH NP bed. The images and the chemical maps were taken on two different spots of the same sample. The maps emphasize the absorption bands of the coordinated −carboxy functions (1650 cm^{-1}), the aromatic linkers (1504 cm^{-1}), and the SiO_2 NP bed underneath the MOF-5 crystals (1200−1000 cm^{-1}).

which in turn allows for the formation of terephthalate bridges connecting the MOF-5 network.[17] The coordination with Zn^{2+} cations is verified by the shift of the main ν_a^{OCO} frequency component from 1610 to 1650 cm^{-1}. As the OCO band is usually very strong and has an almost invariant extinction coefficient (about 1 $mM^{-1}m^{-1}$), it is possible to qualitatively associate its wavenumber shift with the chemical state of the OCO bond.[32] The inductive effects of coordinated metals can be understood in terms of dipole−dipole and charge−dipole interactions, and with a simple empirical consideration, a shift of the OCO frequency toward higher frequencies indicates a stabilization of COO species of the 1,4-benzenecarboxylic acid molecules.[32] In addition to the Zn-coordinated OCO stretch, characteristic symmetric stretch vibrations of the MOF-5 aromatic linkers have been measured at 1504 cm^{-1} (=C−H and ring C=C stretch) and 1015 cm^{-1} (=C−H of para-coordinated aromatic ring). The spatial arrangement of both the organic and inorganic chemical bonds is consistent with the expected distribution of the analyzed species and correlates well with the optical microscope images. Remarkably, the growth rate of MOF-5 was found to be even faster than that observed using NPs suspended in DEF, as after only 2 h the modified substrates showed the presence of the cubic crystals. FTIR mapping confirmed the chemical fingerprint of MOF-5. In support to what observed using FTIR, an XRD analysis of the observed crystals was also performed and reported in the Supporting Information, in Figure SI-5. The crystals had been collected from the substrate as a powder sample and inserted into a glass capillary for this measurement. The obtained pattern is consistent with the one reported for MOF-5.[27]

(31) Lin-Vien, D.; Colthup, N. B.; Fateley, W. G.; Grasselli, J. G. *The Handbook of Infrared and Raman Characteristic Frequencies of Organic Molecules*; Academic Press: San Diego, 1991.
(32) Wright, W. W.; Vanderkooi, J. M. *Biospectroscopy* **1997**, *3*, 457.
(33) Lide, D. R. *The Handbook of Chemistry and Physics*, 84th ed.; CRC press: Boca Raton, FL, 2004.

Conclusion

SiO_2 NPs with carboxy or amino functions can be successfully used as growing seeds to promote MOF-5 formation. Their nucleating capability can be exploited when either suspended in the MOF-5 growing medium or deposited onto a suitable substrate. The extent of the growing surface offered by the NPs emphasizes the heterogeneous nature of MOF-5 crystal formation, speeding their formation rate up to 10 times faster than a conventional one step solvothermal synthesis. The procedure allows for formation of microcrystals with narrow size distribution, with no use of growth inhibitors. As a consequence, this process and the crystals, thus, produced are suitable candidates for the realization of MOF-based devices.

Acknowledgment. Part of this research was undertaken on the FTIR and Powder Diffraction beamlines at the Australian Synchrotron, Victoria, Australia. D.B. acknowledges the Australian Research Council for support through the APD Grant DP0988106. D.B., P.F., and A.J.H. acknowledge the CSIRO OCE Science Leader Scheme for support. John Ward and Mark Greaves are thanked for their expert assistance with the SEM.

Supporting Information Available: SEM imaging, size distribution histograms, and chemical characterization (FTIR) of the SiO_2 NPs modified with carboxy, amino, and hydroxy groups. Optical imaging of the growing batches after 2 h reaction and XRD characterization of the obtained MOF-5 crystals after a 10 h reaction (PDF). This material is available free of charge via the Internet at http://pubs.acs.org.